Transitioning to clean energy transportation services: Life-cycle cost analysis for vehicle fleets

Stephen Comello [a],[*], Gunther Glenk [b], Stefan Reichelstein [b],[a]

[a] *Stanford Graduate School of Business, United States of America*
[b] *School of Business, University of Mannheim, Germany*

ABSTRACT

Comprehensive global decarbonization requires that transportation services cease to rely on fossil fuels for power generation. This paper develops a generic, time-driven life-cycle cost model for mobility services to address two closely related questions central to the emergence of clean energy transportation services: (i) the utilization rates (hours of operation) that determine how alternative drivetrains rank in terms of their cost, and (ii) the cost-efficient share of clean energy drivetrains in a vehicle fleet composed of competing drivetrains. The model compares alternative drivetrains with different environmental and economic characteristics in terms of their life-cycle cost for any given duty cycle. The critical utilization rate that equates any two drivetrains in terms of their life-cycle cost is shown to also provide the optimization criterion for the efficient mix of vehicles in a fleet. This model framework is then calibrated in the context of urban transit buses, on the basis of actual cost- and operational data for an entire bus fleet. In particular, our analysis highlights how the economic comparison between diesel and battery-electric transit buses depends on the specifics of the duty cycle (route) to be served. While electric buses entail substantially higher upfront acquisition costs, the results show that they obtain lower life-cycle costs once utilization rates exceed only 20% of the annual hours, even for less favorable duty cycles. At the same time, the current economics of the service profile examined in our study still calls for the overall fleet to have a one-third share of diesel drivetrains.

1. Introduction

With the transition towards renewable power gaining momentum, the global quest for energy decarbonization is increasingly focused on the transportation sector [1,2]. The impending climate crisis [3, 4], in combination with concerns about local air pollution [5], provide a growing impetus to replace internal combustion engines with zero-emission drivetrains [6]. Yet, the economics of clean energy drivetrains, potentially powered by batteries [7,8], hydrogen [9] or biofuels [10], remains a topic of intense debate for both passenger- and cargo transportation services [11].

The central question addressed in this paper is how a fleet operator should combine alternative drivetrains with different environmental and economic characteristics so as to meet a given transportation service profile in a cost-efficient manner. This question has parallels to the task of combining alternative power generation technologies [12], such as renewable power plants and those based on fossil fuels, in a cost-efficient manner so as to meet a given electricity load profile [13, 14].

One major contribution of this paper is the development of a model framework for identifying cost-efficient vehicle fleets according to a

cost metric called the Levelized Cost per X-mile (LCXM). Applicable to any kind of transportation service (passenger and cargo), the LCXM reflects the unit cost of a transportation service, such as a ton- or passenger-mile delivered. Our unit cost concept of the LCXM is related to the Total Cost of Ownership (TCO), a life-cycle cost metric that has been widely used in transportation studies [15,16] and captures the total discounted cost of acquiring, operating, and selling a vehicle [17,18]. The TCO has been employed in the literature to compare the overall cost of alternative drivetrains at the vehicle level [19,20], and in connection with fleets [21–23].

The LCXM metric extends TCO in the direction of the Levelized Cost of Electricity (LCOE), a unit cost measure commonly used in the energy literature. Our model is predicated on the notion that operating costs are driven by the hours of vehicle operation. This conceptualization of the life-cycle cost of transportation services is in the tradition of time-driven activity based costing systems, a construct that has proven useful in multiple industries, including energy systems and health care [24]. This time-based approach allows a planner to capture not only distance

---

traveled but also other duty cycle characteristics like vehicle speed and stop frequency, all of which have differential cost implications [25,26].

The LCXM metric is shown to yield the cut-off points in terms of annual operating hours that make one drivetrain more economical than another. The cut-off points, in turn, provide the decision criterion for choosing the cost-efficient shares of alternative drivetrains in a fleet that is to meet a given demand schedule or load profile. Thus, the LCXM concept provides a unified framework for examining the (i) cost competitiveness of individual vehicles, (ii) optimal mix of alternative drivetrains in a fleet, (iii) efficient dispatch of alternative drivetrains, and (iv) effect of the characteristics of multi-dimensional duty cycles on the composition of cost-efficient vehicle fleets. Finally, as a life-cycle cost measure, the LCXM also accounts for any environmental externalities that are captured in terms of their pecuniary costs.

The second major contribution of this study is to apply the LCXM model framework in the current economic context of an urban bus service provider in California as a case in point. Urban transit bus fleets have received considerable attention in the transportation literature as well as in the urban planning and policy-making communities [8,27, 28]. Relying on recent measurements of cost and operational performance per bus in the provider's fleet as well as real-time protocols for bus dispatches to routes served, this study specifically contrasts the life-cycle cost of battery-electric buses with that of diesel buses. While the former entail a substantially higher acquisition cost, they result in a lower life-cycle cost compared to diesel buses, provided the annual utilization rate is at least around 1300 hours, with the exact cut-off depending on the characteristics of the particular route served. As a reference point, the average annual utilization of transit buses in the U.S. amounts to 2508 hours [29].

Given the hourly schedule for bus services provided in the context of our application in California, the results show that the share of electric vehicles in a cost-efficient bus fleet currently varies between one and two thirds, depending on the routes to be served. While ongoing trends favor increasing reliance on electric buses within a fleet, conventional drivetrains remain part of a cost-efficient fleet in the California environment for now. The empirical findings provide a cost-based rationale for the transition from conventional diesel buses to battery-electric vehicles in the context of urban transit buses [6,30]. In relation to earlier studies on the economics of clean energy vehicles [15,16], the results point to a more favorable competitive position of electric vehicles [17,19]. Central to the presented analysis is that the efficient share in the overall fleet is determined by the characteristics of the required service load profile.

The paper is structured as follows: Section 2 presents the LCXM model framework, beginning with the life-cycle cost of transportation formulation at a vehicle-level, followed by its extension to a cost-efficient fleet-level analysis. Section 3 then applies these formulations to the California context and yields empirical results. Section 4 discusses the results and presents sensitivity analyses. The paper concludes in Section 5. The Appendix provides formal proofs and details concerning the underlying data used in the empirical analysis.

2. Economic model

2.1. Life-cycle cost of transportation services

The central element of the model developed in this paper is a unit cost measure that is a direct analogue of the familiar *Levelized Cost of Electricity (LCOE)*. This metric serves as the relevant benchmark for comparing the cost of alternative power generation sources, such as natural gas or solar PV. Expressed in dollars per kilowatt hour (kWh), the LCOE is conceptualized as the average unit revenue that an equity investor would require for all kilowatt hours produced to break-even on a particular investment [31]. This unit revenue must cover all operating expenses, repay the project debt, and attain an appropriate return for equity investors [32,33].

For a generic transportation service that carries physical objects across locations, the measure of output will generally be 'X-miles' (or 'X-kilometers' with straightforward conversion). In the context of cargo transports, this measure frequently becomes *ton-miles*, i.e., if on average z tons of cargo are transported for y miles, the vehicle delivers $z \cdot y$ ton-miles. Similarly, in the context of passenger travel, the corresponding measure could be *passenger-miles*. For passenger cars, the appropriate measure may simply be *miles* if the primary purpose of the service is to transport the driver of the vehicle.

Our model is predicated on the notion that operational costs incurred are driven by the total time the vehicle is in operation. For a given T-year planning horizon, we denote by $\vec{h} \equiv (h_1, \ldots, h_T)$ the *usage profile* of a vehicle, where $0 \leq h_i \leq 8,760$ is the utilization in hours of operation in year i (a list of symbols and acronyms is provided in the Appendix). The number of miles traveled in year i is then given by the average velocity in miles/hour, $a(\theta)$, multiplied with h_i. Velocity depends on the characteristics of the *duty cycle*, θ, a multi-dimensional parameter that captures the relevant performance requirements in a specific transportation context. For transit buses, for instance, the duty cycle reflects the specifics of the route, including the number of bus stops per mile, the ambient temperature, and the topography of the route.

The number of passengers or tons of cargo transported in any given year is also determined by the utilization in that year. Allowing for the possibility of a non-linear relation, we let the function $b_i(h_i|\theta)$ represent the average number of passengers or tons transported if the vehicle travels $a(\theta) \cdot h_i$ miles in year i. The total number of X-miles then becomes:

$$X_i(h_i|\theta) = b_i(h_i|\theta) \cdot a(\theta) \cdot h_i.$$

Turning to cost components, let v denote the initial acquisition expenditure for the vehicle. At the end of its useful life, the vehicle may yield a salvage value $\lambda \cdot v$, with $0 < \lambda < 1$. In terms of annual operating costs, we distinguish between variable and fixed costs in year i. The variable component, $w_i(h_i|\theta)$, varies with the hours of operation in year i. Fixed costs, $F_i(\theta)$, are by definition usage-independent. Applicable examples for variable operating costs include fuel, spare parts, and the prorated salary for the driver. In contrast, insurance, registration, and certain maintenance activities are fixed costs. In the specific case of an electric vehicle, the cost of the battery warranty, where the potential replacement cost of the battery during the useful life of the vehicle is 'smoothed' through periodic warranty payments, would be considered a fixed cost.

Aggregation of the different cost components into a single unit cost number requires a 'levelization' factor given by the discounted number of X-miles that the vehicle travels over its useful life. Let r denote the applicable cost of capital that investors require for a project, with $\gamma = \frac{1}{1+r}$ denoting the corresponding discount factor. Then the levelization factor in terms of discounted future X-miles is defined as:

$$Y(\vec{h}|\theta) = \sum_{i=1}^{T} X_i(h_i|\theta) \cdot \gamma^i.$$

A final cost category stems from corporate income taxes and a depreciation tax shield that a firm or individual may be subject to. As shown in the Appendix, this cost category can be summarized, including the potential salvage value, in a factor Δ that adjusts the acquisition cost of the vehicle. Overall, the levelized cost per X-mile is then defined as the sum of three components:

$$LCXM(\vec{h}|\theta) = w(\vec{h}|\theta) + f(\vec{h}|\theta) + c(\vec{h}|\theta) \cdot \Delta, \tag{1}$$

where:

$$c(\vec{h}|\theta) \equiv \frac{v}{Y(\vec{h}|\theta)}, \quad w(\vec{h}|\theta) \equiv \frac{\sum_{i=1}^{T} w_i(h_i|\theta) \cdot \gamma^i}{Y(\vec{h}|\theta)}, \quad f(\vec{h}|\theta) \equiv \frac{\sum_{i=1}^{T} F_i \cdot \gamma^i}{Y(\vec{h}|\theta)}.$$

$$\tag{2}$$

The Appendix formally establishes that the LCXM metric, as defined in (1), does satisfy the break-even criterion that investment in a vehicle has zero net-present value if the average revenue per X-mile delivered is exactly equal to the LCXM.

Claim 1. *For a given duty cycle θ and usage profile $\vec{h}$, the $LCXM(\vec{h}|\theta)$ in (1) is the break-even price per X-mile.*

The LCXM metric yields an immediate cut-off frontier in terms of utilization that makes one drivetrain preferable to another in terms of life-cycle cost. For simplicity, suppose that the variable cost, $w_i(\cdot)$, per hour of operation is constant such that $w_2 > w_1$. If drivetrain 1 involves a higher acquisition cost than drivetrain 2, the former is referred to as 'baseload' and the latter (drivetrain 2) as the 'peaker'. If in each year i the utilization rate h_i exceeds the cut-off utilization rate h^*, the baseload drivetrain will be more cost effective. The critical h^* is given as the unique value that equates the two levelized cost curves, that is:

$$LCXM_1(h^*, \dots, h^*|\theta) = LCXM_2(h^*, \dots, h^*|\theta).$$

Conversely, the peaker drivetrain is preferable from a cost perspective for consistently low utilization rates $h_i < h^*$. Depending on the parameters in the different cost categories, it is, of course, possible that h^* exceeds the annual limit of 8760 h in which case the peaker drivetrain entails lower life-cycle cost irrespective of the actual utilization rates.

2.2. Cost-efficient vehicle fleets

Consider now a service provider that chooses a vehicle fleet composed of multiple drivetrains. Initially, it is supposed that $L(t)$ represents the load profile of vehicles required to operate during the tth hour of every day of the year, in each of the next T years on the same duty cycle θ. Suppose the service provider seeks to minimize the acquisition and ongoing operating costs of two alternative drivetrains. Let k_u denote the number of vehicles of type u. It will be convenient to first ignore the integer constraint on vehicles. Suppose that the maximum value of $L(t)$ on $[0, 24]$ is k_+, and that $L(\cdot)$ can be uniformly approximated by a polynomial function on the interval $[0, 24]$ (Weierstrass Theorem). Thus $k_1 + k_2 \geq k_+$. Finally, let $D(k)$ denote the total amount of time in $[0, 24]$ during which at least k vehicles must be in operation according to $L(\cdot)$. Formally,

$$D(k) \equiv \|\{t \in [0, 24] | L(t) \geq k\}\|, \tag{3}$$

where $\| \cdot \|$ denotes the total length of the intervals for which $L(t) \geq k$. Since $L(\cdot)$ can be described by a polynomial, there are at most finitely many such intervals. By construction, $D(\cdot)$ is continuous and decreasing in k. Furthermore, if $L(\cdot)$ attains its maximum at a unique point in time, the function $D(\cdot)$ assumes all values between zero and 24.

Claim 2. *Consider two drivetrains whose levelized cost curves, $LCXM_1(\cdot)$ and $LCXM_2(\cdot)$, intersect at $(h^*, \dots, h^*)$ with $h^* \in [0, 8760]$. Given the daily load profile $L(t)$, the cost-minimizing number of baseload drivetrains, k_1^*, is given by:*

$$365 \cdot D(k_1^*) = h^*.$$

The intuition for this result (formally demonstrated in the Appendix) is that in order for the total cost associated with the fleet operation to be minimized, the 'marginal' baseload vehicle (drivetrain 1) must operate for exactly $\frac{h^*}{365}$ hours per day. Otherwise the total life-cycle cost could be lowered by either replacing this last vehicle by a peaker or expanding the number of baseload vehicles. Since k_1^* will generally not be an integer, the actual cost-minimizing number of baseload drivetrains will be one of the two integers adjacent to the k_1^* identified in the equation for h^*. This reflects that the overall LCXM associated with the load profile $L(\cdot)$ is a convex combination of the two individual LCXMs.

Table 1
Main cost parameters (in 2019 $US).

	Diesel	Electric
Variable cost per hour (Route A)	$26.25	$2.02
Variable cost per hour (Route B)	$16.79	$4.77
Fixed cost per year	$5,054	$5,913
Net acquisition cost	$425,189	$631,300
Useful lifetime	12 years	12 years
Cost of capital	5.00%	5.00%

The preceding framework is readily extended to settings where each day has its own distinct load profile $L_j(\cdot)$, with $1 \leq j \leq 365$. To that end, suppose that each $L_j(\cdot)$ satisfies the same technical conditions as $L(\cdot)$ above, and denote by $D_j(\cdot)$ the analogue of the function $D(\cdot)$ in (3) corresponding to $L_j(\cdot)$ rather than $L(\cdot)$.

Claim 3. *Under the conditions of Claim 2, if the daily load profiles are given by $L_j(\cdot)$, the cost-minimizing number of baseload drivetrains, k_1^*, is given by:*

$$\sum_{j=1}^{365} D_j(k_1^*) = h^*.$$

3. Application: Transit bus fleets

3.1. Life-cycle cost comparisons

The preceding framework is now applied to the current economic environment of an urban bus service provider as a case in point. Urban bus service providers have been among the first fleet operators to replace diesel-powered vehicles with battery-electric or even hydrogen-electric buses [6]. Stanford University in California initiated this transition a number of years ago. The university provided detailed records of its bus service based on multiple information systems pertaining to energy and fleet management, covering all relevant cost and operational data. The Appendix provides details of both the data and the collection process.

Like a municipal bus service, Stanford's bus service known as *Marguerite* interconnects the university campus and the surrounding community via multiple routes. It operates daily at varying levels of capacity utilization with peaks during weekday mornings and afternoons. The majority of the service is provided with transit buses (see the Appendix). Beginning in 2014, the university has begun to gradually replace diesel-powered with battery-electric buses.

To compare the life-cycle cost of the two drivetrains for different duty cycles, the calculations focus on two distinct routes, referred to as Route A and B. They reflect opposite ends of the range of duty cycles operated by Marguerite, with the number of bus stops per mile at 1.11 and 2.67 and the average velocity at 7.40 and 3.01 miles per hour for Route A and Route B, respectively. Since topography and ambient temperature of all campus routes are virtually identical, Routes A and B generally yield corner solutions for the set of routes operated by Marguerite. While this set reflects common duty cycles for fairly flat topographies in a Mediterranean climate, we might expect regions with more diverse route characteristics to exhibit a wider range of velocity figures.

Table 1 shows average values for the main life-cycle cost components (details provided in the Appendix). The net acquisition cost represents the initial purchasing price minus the salvage value and, for electric buses, a capital incentive of $100,000 granted by the California Air Resources Board [34]. The variable cost comprises fuel costs and variable maintenance costs but excludes the salary of drivers, which is the same across drivetrains. Note that all cost, route and performance measures associated with distance can readily be expressed in terms of kilometers (meters) or miles by using the appropriate conversion factor (1 mile = 1.609 km).
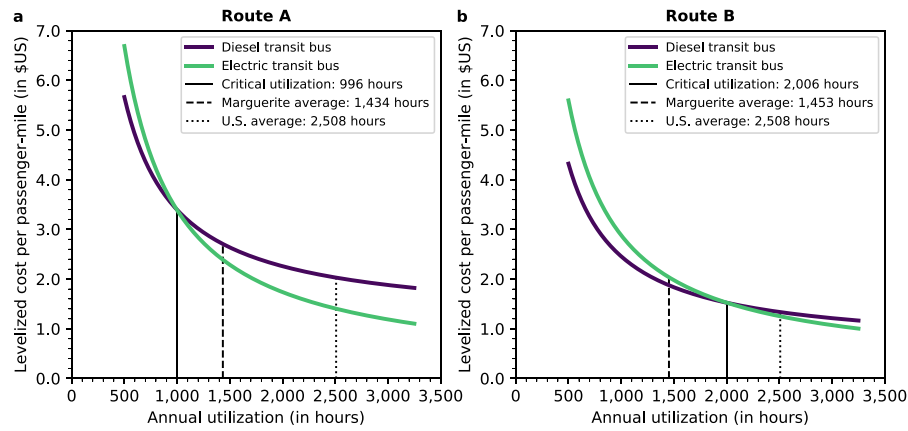
Fig. 1. Levelized cost per passenger-mile. a, b, This figure shows the levelized cost per passenger-mile of diesel and electric transit buses for (**a**) Route A and (**b**) Route B.

Considering the variable costs in Table 1, one might expect that more stops per mile (Route B) increase the variable cost of both drivetrains and especially that of diesel buses whose fuel consumption is more sensitive to frequent stops. Yet, this intuition can be misleading. The increased fuel cost per mile of a diesel bus on Route B is outweighed by the relatively low average velocity resulting in a lower fuel cost per hour of operation. For electric buses, in contrast, the same reasoning applies, yet fuel costs are only a small share of the overall variable cost of operation. The larger component of variable maintenance costs, e.g., brake replacement, is indeed higher on Route B with more stops per mile and therefore the overall variable cost per hour for an electric bus on Route B exceeds that of Route A.

Fig. 1 depicts the levelized cost curves per passenger-mile (LCPM) for both drivetrains by route. Beyond the unique critical utilization value, h^*, electric buses entail a lower life-cycle cost. These cut-off values amount to 996 hours for Route A and 2006 hours for Route B, marked by the solid vertical lines in Fig. 1. The substantially lower cut-off value on Route A mainly reflects that the ratio of the variable costs per hour for the two drivetrains is relatively large on that route. The critical utilization value for the average duty cycle (number of stops per mile) of the entire Marguerite system amounts to 1329 hours; see the Appendix for details.

The operational records of the Marguerite fleet show that Route A is almost exclusively served by electric buses, while the opposite holds for Route B. The average annual utilization factors amount to 1434 hours and 1453 hours, respectively. For these utilization factors, Fig. 1 shows that the LCPM of electric buses is lower than that of diesel buses on Route A, while the opposite pattern applies on Route B. The reliance on these two drivetrains for the two routes thus appears consistent with the goal of minimizing the life-cycle cost of transportation services provided. For further reference, the average annual utilization of transit buses in the U.S. amounts to 2508 hours [29]. Such high utilization rates would give electric buses a cost advantage on both routes, as shown in Fig. 1.

As discussed in the Introduction, the transportation literature has considered alternative output measures for transportation services. In the context of urban bus transport, miles would be a natural alternative to passenger-miles. The corresponding cost curves, denoted by $LCM(·)$, for Routes A and B are shown in Fig. 2. Direct comparison with the cost curves in Fig. 1 shows that when the output measure is passenger-miles both types of drivetrains experience a lower life-cycle cost on Route A in comparison to Route B. Yet, the opposite directional change emerges for $LCPM$. This opposite effect reflects that there are on average three times as many passengers on Route B compared to Route A. At the same time, it should be noted that on both routes the $LCM(·)$ curve decreases more steeply than the $LCPM(·)$ curve. This ranking reflects the general property that, provided $b(·|θ) > 1$, $|LCPM'(h)| < |LCM'(h)|$, for all values of h. At the same time, the critical utilization rate h^* is invariant to the particular measure of X-miles.

3.2. Cost-efficient vehicle fleets

Turning next to fleet-level considerations, Fig. 3 depicts the daily load profiles of buses operating in the Marguerite fleet. If hypothetically all Marguerite buses were to run on Route A, the efficient number of diesel and electric buses would amount to 7 and 22, respectively. The corresponding values for Route B are 18 and 11. Since the functions $D_j(·)$ are decreasing in k_1, the efficient number of electric buses for Route B is smaller than on Route A, as the corresponding critical utilization factor h^* is larger for Route B (see Fig. 1). Though the proportion of the two competing drivetrains within the fleet differ significantly for Routes A and B, diesel buses will be dispatched only within the 'rush-hour' periods corresponding to peak demand. The load profile depicted in Fig. 3 is an overlay of the hourly profile for individual days in 2019. The more the daily profiles overlap, the darker is the shade of gray. The upper twin peaks represent load profiles on weekdays, while the lower twin peaks display the profile for weekend days.

If the number of stops per mile is taken to be the average of all routes served by Marguerite and all buses were to serve that average route, the optimal number of diesel and electric buses would be 11 and 18. For this scenario, electric buses would be operating as baseload capacity for more than the respective h^* hours per year, whereas each of the diesel buses would be operating as peakers for less than that. An insight from our analytical framework is that it will generally be efficient to have a mix of baseload and peaker vehicles, unless the underlying load profile assumes an 'extreme' shape. Specifically, even if all serviced routes were to correspond to the characteristics of Route B, which tend to favor diesel buses, a planner would still want to procure 11 electric buses out of a total of 29. That share would, of course, be even larger if the load profile in Fig. 3 was less 'peaky' and replaced by a more uniform service schedule.

The model of fleet optimization presented in this paper has ignored requirements for backup capacity due to the possibility of unscheduled vehicle maintenance or the occurrence of special events in the service area. In fact, the Marguerite fleet currently includes 10 transit buses over and above the annual peak demand of 29 scheduled buses. The average utilization rate for buses on both routes is therefore even further below the U.S. average. At the same time, given that the Marguerite fleet already included 29 electric buses in 2019, the university will lower its total operating costs by reducing its reliance on diesel buses to the largest extent possible.

4. Discussion

The preceding numerical calibration of the life-cycle cost of transit buses relies on the recent data records of a single service operator. It is therefore essential to examine the sensitivity of the findings to changes
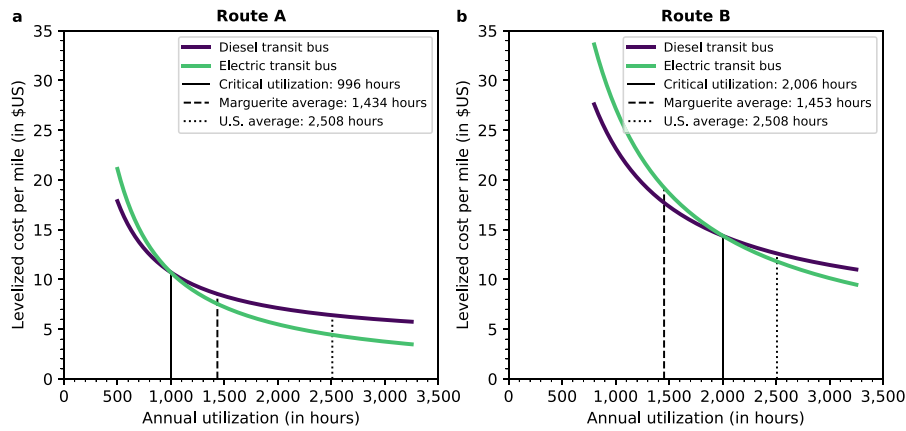
Fig. 2. Levelized cost per mile. a, b, This figure shows the levelized cost per mile of diesel and electric transit buses for (**a**) Route A and (**b**) Route B.
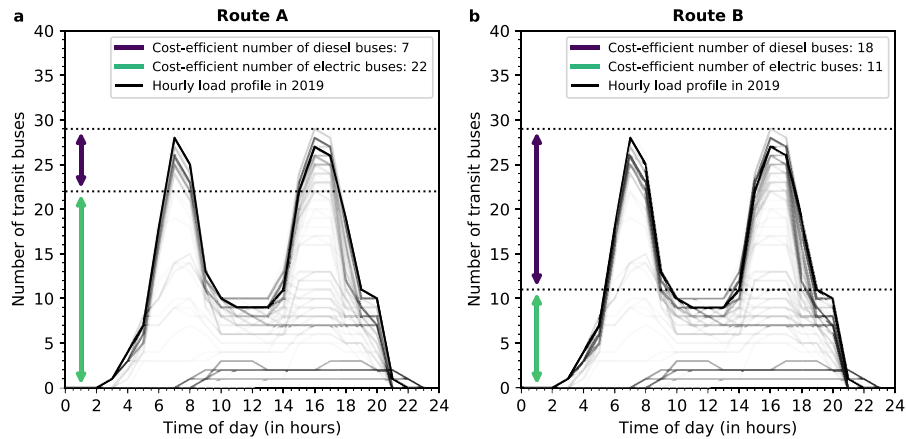

Fig. 3. Cost-efficient vehicle fleets. a, b, This figure shows the cost-efficient number of diesel and electric transit buses for the hourly load profile of Marguerite in 2019 if, hypothetically, all routes exhibited a duty cycle of either (**a**) Route A and (**b**) Route B.

in the key input variables pertaining to other economic environments, changes in public policy, and general economic trends.

The graphs in Fig. 4 focus on the sensitivity of the critical utilization rate, i.e., $\frac{h^*}{8760}$, as derived in Fig. 1 and the efficient share of electric buses, i.e., $\frac{k_1^*}{29}$, as derived in Fig. 3. The comparisons focus on the same two routes in order to illustrate the impact of alternative duty cycles.

Electricity rates differ substantially across jurisdictions. Yet, the purple lines in Fig. 4 indicate that both dependent variables (h^* and k_1^*) are insensitive to changes in the electricity cost of electric buses, as they constitute only a minor share of the overall life-cycle cost of electric buses.

In contrast, the blue lines in Fig. 4 show that the dependent variables are sensitive to changes in the fuel cost of diesel buses. The cost of diesel fuel fluctuates over time and across geographic regions. In addition, diesel fuel may become subject to CO_2 emission charges in some jurisdictions. Quantifying the overall effect, the blue lines in Fig. 4 show that a 20% increase in the fuel cost of diesel buses will decrease the critical utilization rate by about 12%–18%, depending on the route. The corresponding impact on the efficient share of electric buses would be more pronounced on Route B and result in an increase of k_1^* by about 10%.

Any increases in the cost of capital should intuitively weaken the competitive position of electric buses, that is h^* to increase and k_1^* to decrease. While the LCPM of both drivetrains will increase, a larger cost of capital should have a more pronounced effect on the more capital-intensive drivetrain, i.e., electric vehicles. A similar observation emerges in connection with capital-intensive renewable energy in comparison to fossil fuel power plants [35]. The yellow lines in Fig. 4

confirm this intuition, though the changes in the dependent variables turn out to be relatively minor on both routes, and for both variables. Specifically, the critical utilization rate increases almost linearly at the modest rate of 3% for every 10% increase in the cost of capital.

Recent advances in lithium-ion battery technology have significantly lowered the price of lithium-ion battery packs, which, in turn, comprise a significant share of the net acquisition cost of battery electric buses [36]. Numerous recent studies point to sustained cost reductions in the future along the trajectory of a classic learning curve [6,37,38]. An additional development that is forecast to lower the net acquisition cost of battery electric buses is the emergence of a market for 'second-life' battery applications [39,40], once the degradation of the battery packs makes them no longer suitable for transportation services. In the context of the model presented here this would increase the salvage value with a corresponding decrease in the net acquisition cost of electric buses. The green lines in Fig. 4 confirm that the critical utilization rate is highly sensitive to increases in the net acquisition cost of electric buses. On either route, a 10% change in the net acquisition cost results in approximately a 30% change in h^*.

Naturally, the efficient share of electric vehicles is decreasing in the net acquisition cost of electric vehicles. These decreases occur at a lower rate on Route A (Fig. 4c) compared to Route B (Fig. 4d), which exhibits a larger difference in the hourly operating costs of the two drivetrains. From a public policy perspective, the finding is that without the current $100,000 capital subsidy made available to electric buses by the California Air Resource Board, the efficient share of electric vehicles in the Marguerite fleet would decrease by about 25%. Yet, if the net acquisition cost of electric vehicles were to drop by 40%,
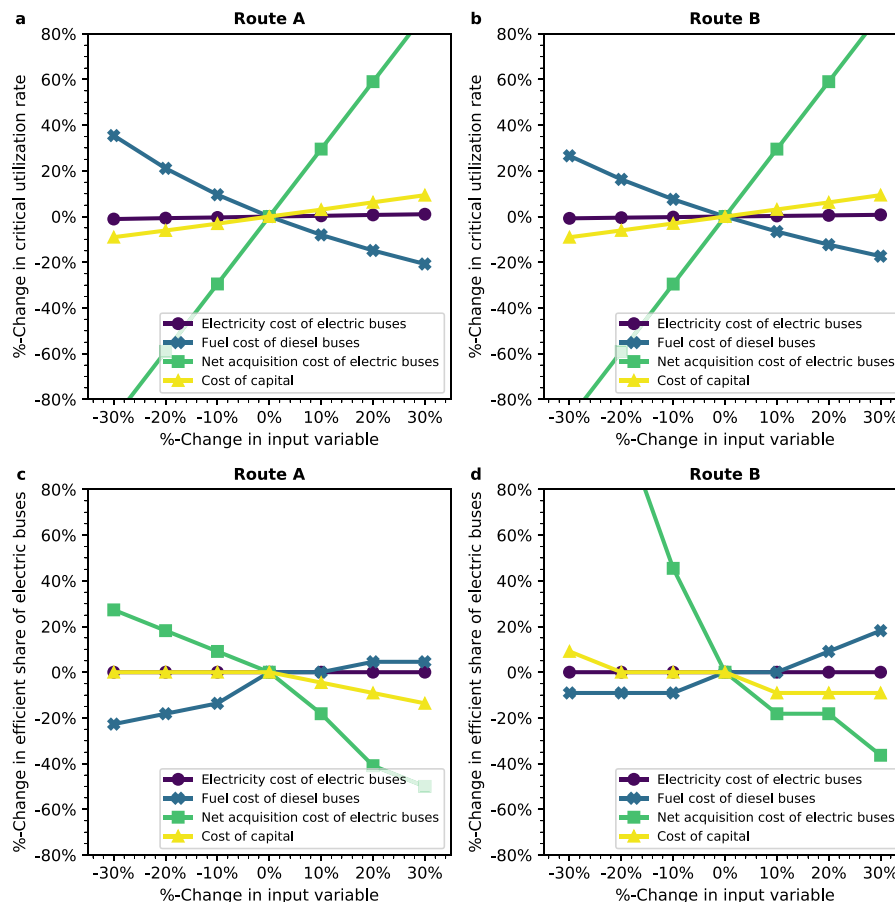
Fig. 4. Sensitivity analysis. a, b, c, d This figure shows the sensitivity of the critical utilization rate on (**a**) Route A and (**b**) Route B, as well as the sensitivity of the efficient share of electric buses on (**c**) Route A and (**d**) Route B to four different input variables.

then an all electric bus fleet would be cost-minimizing on both routes. Based on current price trajectories for lithium-ion battery packs [37,41] and conservatively estimating that such packs constitute 30% of the net acquisition cost, this scenario should emerge no later than the year 2025.

5. Conclusions

In many industrialized countries, the efforts to decarbonize the economy are increasingly focused on the transportation sector. This paper has developed a time-driven life-cycle cost model for mobility services. The model yields a ranking of alternative drivetrains with different environmental and economic characteristics in terms of their life-cycle cost for any given duty cycle. The critical utilization rate that equates any two drivetrains in terms of their life-cycle cost is shown to also provide the optimization criterion for the efficient mix of the competing drivetrains in a vehicle fleet. In sum, the levelized cost model developed here provides a unified framework for examining the (i) cost competitiveness of individual vehicles, (ii) optimal mix of alternative drivetrains in a fleet, (iii) efficient dispatch of alternative drivetrains, and (iv) effect of the characteristics of multi-dimensional duty cycles on the composition of cost-efficient vehicle fleets.

The LCXM metric is calibrated and applied in the context of an urban bus service as a case in point, where the output measure is either miles traveled or passenger-miles delivered. The findings of this empirical analysis still point to a significant role for diesel buses during peak demand across all types of routes. The critical utilization quantity is highly dependent on route-specific characteristics, and so is the economically efficient proportion of electric drivetrains within a fleet that is required to meet a given load profile. At the same time, the

optimal share of diesel buses within a fleet is forecast to diminish substantially in the next five years, provided recent improvements in electric drivetrains continue.

Regarding future work, it will be instructive to extend and apply the framework to a broader array of drivetrain technologies, including hydrogen fuel cells and biofuels. The framework is also applicable to a range of transportation modes, including passenger- and cargo transports by road, water and air. In the context of passenger road vehicles, the recent advances in mobility-as-a-service suggest that the traditional ownership model will increasingly be replaced by fleet ownership. This trend and the wider adoption of clean energy vehicles are likely to reinforce each other on account of higher utilization rates associated with vehicle sharing and the comparatively lower operating costs of clean energy vehicles.

CRediT authorship contribution statement

Stephen Comello: Conceptualization, Methodology, Data curation, Formal analysis, Writing - original draft, Writing - review & editing, Project administration, Investigation, Software. **Gunther Glenk:** Conceptualization, Methodology, Data curation, Formal analysis, Writing - original draft, Writing - review & editing, Project administration, Investigation, Software, Visualization. **Stefan Reichelstein:** Conceptualization, Methodology, Writing - original draft, Writing - review & editing, Project administration, Formal analysis.

Declaration of competing interest

The authors declare that they have no known competing financial interests or personal relationships that could have appeared to influence the work reported in this paper.

Appendix

List of symbols and acronyms

Variable	Unit	Description
α	%	Corporate income tax rate
Δ	–	Tax factor
γ	–	Discount factor
λ	%	Share of acquisition cost as salvage value
θ	–	Description of duty cycle
$a(\theta)$	miles/h	Average velocity
$b_i(h\vert\theta)$	passengers or tons	Passengers or mass transported in year i
$c(h\vert\theta)$	\$/X-mile	Levelized acquisition cost
CFL_i^o	\$	Annual pre-tax cash flow in year i
d_i	–	Depreciation factor in year i
$D(k)$	h	Duration that $\geq k$ vehicles must operate
$f(h\vert\theta)$	\$/X-mile	Levelized fixed cost
$F_i(\theta$	\$/year	Fixed operating cost in year i
$H(k_i)$	h	Daily operating hours of a drivetrain i
h_i	h	Hours of operation in year i
$\vec{h}$	h	Usage profile
I_i	\$/year	Taxable income in year i
k	–	Number of vehicles
$L(t)$	in k	Load profile per hour t
LCM	\$/mile	Levelized cost per mile
$LCOE$	\$/kWh	Levelized cost of electricity
$LCPM$	\$/passenger-mile	Levelized cost per passenger-mile
$LCXM$	\$/X-mile	Levelized cost per X-mile
kWh	–	Kilowatt hour
p	\$/X-mile	Revenue attained per X-mile
r	%	Interest rate
T	years	Useful lifetime of a given vehicle
TCO	\$	Total cost of ownership
v	\$	Acquisition cost of the vehicle

Variable	Unit	Description
$w_i(h\vert\theta)$	\$/year	Variable operating cost in year i
$w(h\vert\theta)$	\$/X-mile	Levelized variable operating cost
$X_i(\vec{h}\vert\theta)$	X-mile	Output measure in year i
$Y(\vec{h}\vert\theta)$	X-miles	Levelization factor

Details of the economic model

We first complete the description of the model and then validate the formal claims in the main text. The tax factor, Δ, depends on both the applicable income tax rate, denoted by α, as well as the allowable depreciation schedule for tax purposes. That schedule is denoted by $\{d_t\}_{t=1}^T$, such that $d_t \geq 0$ and $\sum_t d_t = 1$, and determines how the initial investment is amortized for tax purposes over time. The overall effect of income taxes can be summarized by:

$$\Delta = \frac{1 - \alpha \cdot \left[\sum_{t=0}^{T} d_t \cdot \gamma^t\right]}{1 - \alpha} - \lambda \cdot \gamma^T. \tag{4}$$

In case $\alpha = 0$, as applicable for a non-profit organization like Stanford University, the tax factor reduces to $\Delta = 1 - \lambda \cdot \gamma^T$.

Proof of Claim 1. Suppose every X-mile attains a revenue of p. For a given duty cycle θ and usage profile $\vec{h}$, we demonstrate that the investment breaks even whenever $p = LCXM(\vec{h}\vert\theta)$. In year i, the operating revenue is given by:

$$Rev_i(h_i) = X_i(h_i\vert\theta) \cdot p = b_i(h_i\vert\theta) \cdot a(\theta) \cdot h_i \cdot p.$$

The overall pre-tax cash flow in year i will be represented by CFL_i^o. It comprises operating revenues and operating costs:

$$CFL_i^o(h_i\vert\theta) = X_i(h_i\vert\theta) \cdot p - w_i(h_i\vert\theta) - F_i(h_i\vert\theta).$$

The firm's taxable income in year i is given by:

$$I_i(h_i\vert\theta) = X_i(h_i\vert\theta) \cdot p - w_i(h_i\vert\theta) - F_i(h_i\vert\theta) - v \cdot d_i.$$

The present value of all after-tax cash flows is therefore given by:

$$\sum_{i=1}^{T} [CFL_i^o(h_i\vert\theta) - \alpha \cdot I_i(h_i\vert\theta)] \cdot \gamma^i - v + (1-\alpha) \cdot \lambda \cdot v \cdot \gamma^T. \tag{5}$$

Direct substitution shows that the expression in (5) is equal to zero if and only if:

$$(1-\alpha) \sum_{i=1}^{T} CFL_i^o(h_i\vert\theta) \cdot \gamma^i + \alpha \cdot \sum_{i=1}^{T} v \cdot d_i \cdot \gamma^i + (1-\alpha) \cdot \lambda \cdot v \cdot \gamma^T = 0. \tag{6}$$

Dividing by $(1-\alpha)$ and recalling the definition Δ, the equality in (6) reduces to:

$$\sum_{i=1}^{T} [X_i(h_i\vert\theta) \cdot p - w_i(h_i\vert\theta) - F_i(h_i\vert\theta)] \cdot \gamma^i = v \cdot \Delta. \tag{7}$$

By definition $Y(\vec{h}\vert\theta) = \sum_{i=1}^{T} X_i(h_i\vert\theta) \cdot \gamma^i$ and therefore (7) holds if and only if $p = LCXM(\vec{h}\vert\theta)$. □

Proof of Claim 2. Given the load profile, $L(\cdot)$, the required total annual number of operating hours becomes:

$$\hat{h} = 365 \cdot \int_0^{24} L(t)\, dt.$$

For any feasible fleet composition, i.e., (k_1, k_2) such that $k_2 \geq k_+ - k_1$, the fleet operator will rely to the extent possible on the drivetrain with the lower unit operating cost. Specifically, the number of daily operating hours of drivetrain 1 will be:

$$H(k_1) \equiv \int_0^{24} \min\{L(t), k_1\}\, dt.$$

The overall cost minimization problem then is to choose k_1 so as to minimize the break-even price p per X-mile required to cover the fleet operator's total life-cycle cost in meeting the daily load profile $L(\cdot)$. In particular, p must satisfy the inequality:

$$
\sum_{i=1}^{T} p \cdot X(\hat{h}) \cdot \gamma^i \geq v_1 \cdot k_1 + v_2 \cdot (k_+ - k_1)
$$

$$
+ \sum_{i=1}^{T} \left[365 \cdot (w_1 \cdot H(k_1) + w_2 \cdot (\hat{h} - H(k_1))) \right.
$$

$$
+ \left. F_1 \cdot k_1 + F_2 \cdot (k_+ - k_1) + \alpha \cdot I_i(\hat{h}, k_1, p) \right] \cdot \gamma^i \quad (8)
$$

$$
- \gamma^T \cdot (1 - \alpha) \cdot \lambda \cdot (v_1 \cdot k_1 + v_2 \cdot (k_+ - k_1)).
$$

Here $I_i(\hat{h}, k_1, p)$ denotes the taxable income in year i, that is:

$$
I_i(\hat{h}, k_1, p) \equiv p \cdot X(\hat{h}) - 365[w_1 \cdot H(k_1) + w_2 \cdot (\hat{h} - H(k_2))]
$$

$$
- F_1 \cdot k_1 - F_2 \cdot (k_+ - k_1) - [v_1 \cdot k_1 + v_2 \cdot (k_+ - k_1)] \cdot d_i.
$$

Recalling the definition of Δ and collecting terms, the above inequality reduces to:

$$
p \geq \frac{1}{\sum_{i=1}^{T} X(\hat{h}) \cdot \gamma^i} \left[v_1 \cdot \Delta \cdot k_1 + v_2 \cdot \Delta \cdot (k_+ - k_1) \right.
$$

$$
+ \sum_{i=1}^{T} \left[365 \cdot (w_1 \cdot H(k_1) + w_2 \cdot (\hat{h} - H(k_1))) \right. \quad (9)
$$

$$
+ \left. \left. F_1 \cdot k_1 + F_2 \cdot (k_+ - k_1) \right] \cdot \gamma^i \right].
$$

To minimize p, we differentiate the right-hand side of (9) with respect to k_1, noting that

$$
H'(k_1) = \int_{\{t \in [0,24] | L(t) \geq k_1\}} dt \equiv D(k_1).
$$

This derivative is given by:

$$
\frac{1}{\sum_{i=1}^{T} X(\hat{h}) \cdot \gamma^i} \left[v_1 \cdot \Delta + \sum_{i=1}^{T} [w_1 \cdot 365 \cdot D(k_1) + F_1] \cdot \gamma^i - v_2 \cdot \Delta - \sum_{i=1}^{T} [w_2 \cdot 365 \cdot D(k_1) + F_2] \cdot \gamma^i \right].
$$

With the duty cycle θ held fixed, we simplify the notation for the levelized cost of passenger-miles by suppressing the dependence on θ. Also, on the domain of utilization profiles that are constant across years, i.e., $h_i = h$, we write $LCXM(h)$ instead of $LCXM(h, \ldots, h)$. Recalling the definition of the LCXM, the last expression for the derivative of the right-hand side of (9) is proportional to:

$$
LCXM_1(365 \cdot D(k_1)) - LCXM_2(365 \cdot D(k_1)). \quad (10)
$$

For a cost minimum, k_1 must be chosen so that the derivative expression in (10) is zero, which implies $k_1 = k_1^*$, since k_1^* is such that $365 \cdot D(k_1^*) = h^*$ and $LCXM_1(h^*) = LCXM_2(h^*)$. Furthermore, since $w_2 > w_1$ and $D(\cdot)$ is decreasing in k_1, the objective function on the right hand-side of (9) is convex in k_1. Thus the value of k_1 that satisfies the first-order condition corresponding to (10) also yields the global cost minimum. ☐

We observe that the levelized cost of the optimized fleet can be expressed as a convex combination of the two component LCXM, with the respective weights given by the respective operating hours of the two drivetrains. For simplicity, suppose that $b_i(h_i) = b$. Referring back to (9), it is then straightforward to verify that the LCXM of the optimized fleet is equal to:

$$
LCXM(365 \cdot \hat{h}) = \frac{365 \cdot H(k_1^*)}{\hat{h}} \cdot LCXM_1(365 \cdot H(k_1^*))
$$

$$
+ (1 - \frac{365 \cdot H(k_1^*)}{\hat{h}}) \cdot LCXM_2(365 \cdot (\hat{h} - H(k_1^*))). \quad (11)
$$

Proof of Claim 3. The proof mirrors that of Claim 2. The total number of vehicles acquired now becomes k_+ given by the maximum value

across all $L_j(\cdot)$. With regard to the expression in (8), the only change is that the variable operating costs now become:

$$
\sum_{i=1}^{T} [w_1 \cdot \sum_{j=1}^{365} H_j(k_1) + w_2 \cdot \sum_{j=1}^{365} (\hat{h}_j - H_j(k_1))] \cdot \gamma^i,
$$

where

$$
\hat{h}_j = \int_0^{24} L_j(t)\, dt \quad \text{and} \quad H_j(k_1) \equiv \int_0^{24} \min\{L_j(t), k_1\}\, dt.
$$

The claim then follows by proceeding exactly as in the preceding proof. ☐

Usage and cost data

The data on input usage and cost items are furnished by various information systems at Stanford University related to energy and fleet management. Table 2 provides the general specifications for the two types of buses considered in our analysis.

Variable and Fixed Costs

Stanford Transportation provided detailed operational cost data. Variable operating and fixed operating costs, as defined in Section 2 of the manuscript, are aggregate cost categories provided in Table 3. For each cost category, its applicability is indicated depending on the drivetrain. This table also shows our classification in terms of variable versus fixed operating costs. This classification was confirmed by the analysts at Stanford Transportation.

Table 4 provides average values for route-invariant cost parameters for both diesel and electric buses. The acquisition cost shown there for each bus type reflects the most recent purchase price. If the purchase occurred before the year 2019, we adjusted the price for inflation with an average annual inflation rate of 2.00%. The capital incentive for electric buses is a subsidy granted by the California Air Resources Board under the Hybrid and Zero-Emission Truck and Bus Voucher Incentive Program [34]. The salvage value for each drivetrain is based on an estimate provided by Stanford. To assess the fixed operating costs of a bus, we took the drivetrain-specific average across transit buses in the Marguerite fleet of annual operations and maintenance costs for the years 2017–2019. The annual fixed cost of each bus comprises the sum of registration fees, insurance cost, and components of maintenance costs that are usage-independent, as shown in Table 3. Further, the annual warranty payment for the battery is considered a fixed cost. The labor cost per hour includes the cost of the driver per hour of operation, composed of salary, benefits, and overhead. Our estimate of the fuel costs is based on the average of diesel prices per gallon paid for the Marguerite fleet in 2019.

The cost of electricity charging for electric buses deserves particular attention. Stanford purchases electricity from a variety of sources each entailing a specific set of fixed, demand and volumetric charges. The total of these electricity costs in 2019 normalized by the total volume of electricity delivered (kWh) amounts to ¢9.20/kWh, which represents the average cost of electricity to the university on a volumetric basis. This cost figure is charged to all administrative units within the university for the consumption of electricity. In addition, each unit is charged a markup for various overhead cost items, resulting in a total of ¢15.20/kWh [42]. For the purpose of determining the life-cycle cost of electric buses, we only impute the normalized volumetric rate, and exclude the university-wide overhead charge, as the former is the effective incremental cost per kWh to the university.

A time-invariant volumetric charge for electricity seems appropriate given the configuration of Stanford's energy system. While the campus as a whole is subject to demand charges and time-of-use volumetric charges, these time-dependent costs are essentially not relevant to the various operating units, including the bus depot, due to the dominance of the university's central energy facility. The facility manages the district heating and cooling for the entire campus and is, therefore,

Table 2

General specifications for the examined buses.

Specification	Diesel	Electric
Make	Gillig MA	BYD K9 Electric Bus
Vintage (year & number)	2003 (8)	2013 (1), 2014 (10), 2017 (18)
Gross Vehicle Weight [lbs]	39,600	40,786
Length [ft]	35.00	35.80
Passenger Capacity	32	34
Drivetrain	Cummins ISB 5.9L I6; 235 hp; 460 lb-ft torque	AC synchronous motor; 80 kW, 350 kWh iron-phosphate battery

Table 3

Variable and fixed cost categories per drivetrain.

Cost category	Diesel	Electric	Cost type
HVAC	Yes	Yes	Fixed
Air Intake System	Yes	No	Fixed
Brakes	Yes	Yes	Variable
Cab-Sheet Metal	Yes	Yes	Fixed
Charging System	Yes	Yes	Fixed
Clean-up/ Detailing	Yes	Yes	Fixed
Cooling System	Yes	Yes	Variable
Cranking System	Yes	Yes	Variable
Diesel Exhaust Fluid	Yes	No	Variable
Tires	Yes	Yes	Variable
Dry Freight Body	Yes	Yes	Fixed
Electric Prop. System	No	Yes	Variable
Electrical Access.	Yes	Yes	Fixed
Exhaust System	Yes	No	Variable
Expendables	Yes	Yes	Variable
Frame	Yes	Yes	Fixed
Front Axle-Susp-Brgs	Yes	Yes	Variable
Fuel System	Yes	No	Variable
General Accessories	Yes	Yes	Variable
Horn-mounting	Yes	Yes	Fixed
Ignition System	Yes	No	Fixed
Instruments	Yes	Yes	Fixed
Liftgate	Yes	Yes	Fixed
Lighting System	Yes	Yes	Fixed
Lines	Yes	Yes	Fixed
Main Auto Trans	Yes	No	Variable
Mounted Equip Repair	Yes	Yes	Fixed
Oil	Yes	No	Variable
Power Plant	Yes	Yes	Fixed
Radio	Yes	Yes	Fixed
Rear Axle-Susp-Brgs	Yes	Yes	Variable
Rear Door	Yes	Yes	Fixed
Refrig-Mechanical	Yes	Yes	Variable
Satellite/Veh Comm	Yes	Yes	Fixed
Special	Yes	Yes	Fixed
Steering	Yes	Yes	Variable
Suppl Info Devices	Yes	Yes	Fixed
Towing	Yes	Yes	Variable
Trim	Yes	Yes	Fixed
Valves	Yes	Yes	Variable
Wash	Yes	No	Fixed
Wheels-Rims-Hubs	Yes	Yes	Variable

Table 4

Route-invariant cost parameters (in 2019 $US).

	Diesel	Electric
Acquisition cost	$430,757	$750,000
Capital incentive	–	$100,000
Salvage value	$10,000	$38,750
Fixed cost per year	$5,054	$5,913
Labor cost per hour	$71.00	$71.00
Fueling cost per gallon	$3.40	–
Charging cost per kWh	–	¢9.20
Useful lifetime	12years	12years
Cost of capital	5.00%	5.00%

Table 5

Route-specific cost parameters (in 2019 $US).

	Route A	Route B	Average
Diesel			
Variable maintenance cost per hour	$5.09	$8.37	$7.04
Energy consumption per hour (in gallons)	6.23	2.48	4.44
Fueling cost per hour	$21.16	$8.42	$15.07
Variable cost per hour	$26.25	$16.79	$22.11
Electric			
Variable maintenance cost per hour	$1.18	$4.46	$3.13
Energy consumption per hour (in kWh)	9.13	3.34	9.01
Charging cost per hour	$0.84	$0.31	$0.83
Variable cost per hour	$2.02	$4.77	$3.96

demand for power in response to time-based price signals, thus enabling the campus to minimize both demand and time-of-use charges [14]. We note that time-invariant volumetric charges for electric buses have also been imputed in other settings applicable to university campuses and municipal bus fleets [43].

The variable cost components include certain maintenance and energy costs, whereby the latter is the product of the route-specific energy consumption and the fueling or charging rate provided in Table 4. Our dataset includes the variable maintenance costs and energy consumption per transit bus in the Marguerite fleet for the years 2017–2019 on the specific days these costs were incurred. These variable cost components vary by route depending on the number of stops per mile and the collection of routes served by a bus throughout the year. The number of buses assigned to each route was assumed to be constant across the years.

Table 5 provides average values for the variable cost for both drivetrains by route. Table 3 shows which categories of the maintenance cost are considered to be usage-dependent for each drivetrain. For Route A, for instance, the average variable maintenance cost is calculated by taking the average across buses for which the annual average number of bus stops per mile is equal to that of Route A.

Route-specific energy consumption for electric and diesel drivetrains are calculated according to different methods which reflect differences in the availability of data. For electric buses, we rely on daily total net energy consumption, total time in service, and total distance traveled as provided by the battery management system for individual buses. Net energy consumption in this context refers to the total energy provided to the bus from the battery minus the energy generated via regenerative braking. We gathered the three categories of the battery management system data for electric transit buses that operated on Route A and B most frequently in 2019. To account for daily and seasonal variation, we attained for each bus a complete battery management system record for a randomly selected day in each month between January–August 2019. This produced 24 records (3 bus readings per month for 8 months) per route. The figures shown in Table 5 for electric buses represent the route-specific average of the 24 measures. The time component of this measure accounts for the actual time a bus was servicing a route. This includes in-service idling but not mid-day lulls when the bus was not in service. As a point of reference, the energy consumption per hour presented in Table 5 corresponds to a power consumption of 1.41 kWh/mi and 1.11 kWh/mi for Routes A and B, respectively.

by far the largest single source of electricity demand, dwarfing, in particular, the incremental load associated with bus charging. The central energy facility has effectively the ability to ramp the university's

Table 6
Stanford Transportation transit bus system route data.

Route	Stops/mile	Velocity [mph]	Passenger/h	Passenger-mile/passenger
A	1.11	7.44	23	1.00
B	2.67	3.01	40	0.70
C	1.35	8.54	19	1.20
D	0.80	21.21	20	2.55
E	1.21	10.82	22	1.50
F	1.21	8.89	14	3.00
G	1.67	7.20	55	1.10
H	1.96	7.89	24	2.50
I	2.50	10.91	50	1.20
J	2.67	8.18	103	1.00
K	1.67	6.55	38	1.20
L	1.74	7.89	24	2.80
M	2.50	8.00	81	1.20
N	2.00	8.00	31	1.20
O	2.70	8.21	15	1.20

Table 7
Route A, Route B and Marguerite average data.

	Route A	Route B	Average
Number of bus stops per mile	1.11	2.67	1.89
Average velocity (in miles per hour)	7.40	3.01	8.70
Average number of passengers	3.15	9.44	6.92
Marguerite average utilization (in h)	1434	1453	1607

For diesel buses, we calculate energy consumption per bus by dividing the total volume (in gallons) dispensed during each refueling event to a specific bus by the total number of in-service hours of the bus within the time interval since the last refueling event for all refueling events recorded in 2019. The corresponding set of bus stops per mile for each bus is calculated based on the duty cycles performed during the same in-service time intervals. The figures in Table 5 result from taking the mean of the calculated per-bus energy consumption measures corresponding to those buses that exhibited stops per mile measures similar to Route A or Route B, winsorized at the 5.00% level. Since the refueling data includes the entire year 2019, the average consumption values account for variations across days, seasons, and vehicles. For reference, the energy consumption per hours given in Table 5 correspond to a fuel economy of 5.26 miles per gallon and 2.61 miles per gallon for Routes A and B, respectively. These values are relatively low because they account for fuel consumed during in-service idling and unplanned maintenance that require idling for troubleshooting.

Route information

Route data for the Stanford Marguerite transit bus system examined in Section 3, including system map and bus stop locations, is found at the Stanford Transportation website. Route information, including the number of bus stops per mile, the average velocity, average number of passengers per hour, and the average number of passenger-miles per passenger is provided in Table 6. Note that actual route names found on the Stanford Transportation site have been anonymized in an effort to maintain a basic level of data security and privacy.

Table 7 provides the main route characteristics for Route A and B, as well as the simple average for these parameters across all routes in the system. The number of bus stops per mile is calculated by dividing the total route distance by the number of bus stops. Finally, average velocity is determined by dividing the total route distance by the expected completion time as provided by Stanford Transportation.

In Table 7, the average number of passengers represents the number of passengers transported across the full distance of a route. This value is the average number of passengers per hour multiplied with the average passenger-miles per passenger and dividing this product by the average velocity. The number of passengers per hour, in turn, is determined by dividing the annual number of passengers that traveled a particular route by the annual total number of hours that the route was serviced. The average passenger-miles per passenger is estimated due to a lack of detailed on-boarding and off-boarding events per passenger as the expected distance in miles that the average passenger would travel on a given route. This figure is defined as the average distance between the two most "popular" bus stops on a route, i.e., the bus stops on a route that have the highest total number of passengers boarding over

the course of a year. Since bus routes are loops that begin and end at the same location, the average distance can be conceptualized as the average length of the two arcs that connect two points on a circle.

For the average utilization, we first calculate the operating hours of each bus in 2019 as the product of the total number of loops per route that a bus accumulated in 2019 with the expected completion time per route. Since we only have data on bus-route assignments for the year 2019, we calculate the operating hours of each bus in 2017 and 2018 by scaling the respective value for 2019 with the total miles that a bus traveled 2017 and 2018. The average utilization per route shown in Table 7 is calculated as follows: for Route B, for instance, one takes the average of all buses that have an average number of bus stops per mile equal to that of Route B. For the system average, the average utilization is the average across all transit buses.

The two routes A and B yield extreme findings for the range of routes operated by Marguerite, because they entail the highest and lowest average fuel consumption per hour observed for diesel buses in the data set. Other routes of the system entail values in between, with the system average amounting to 4.44 gallons per hour. This can largely be attributed to the observation that more bus stops per mile reduce the average miles per hour traveled on a route. Route A exhibits one of the highest values for average velocity, while the opposite holds for Route B. In contrast to the relatively small energy cost of electric buses, the fuel cost for diesel buses becomes the dominant factor in determining the critical utilization rate and, by implication, the cost-minimizing composition of the bus fleet (see Fig. 4).

References

[1] Needell ZA, McNerney J, Chang MT, Trancik JE. Potential for widespread electrification of personal vehicle travel in the United States. Nat Energy 2016;1(9):16112. http://dx.doi.org/10.1038/nenergy.2016.112.

[2] IEA. Global EV outlook 2019. 2019, p. 232. http://dx.doi.org/10.1787/35fb60bd-en, URL: https://www.oecd-ilibrary.org/content/publication/35fb60bd-en.

[3] Knobloch F, Hanssen SV, Lam A, Pollitt H, Salas P, Chewpreecha U, et al. Net emission reductions from electric cars and heat pumps in 59 world regions over time. Nat Sustain 2020;3:437–47. http://dx.doi.org/10.1038/s41893-020-0488-7.

[4] He X, Zhang S, Wu Y, Wallington TJ, Lu X, Tamor MA, et al. Economic and climate benefits of electric vehicles in China, the United States, and Germany. Environ Sci Technol 2019;53(18):11013–22. http://dx.doi.org/10.1021/acs.est.9b00531.

[5] Liang X, Zhang S, Wu Y, Xing J, He X, Zhang KM, et al. Air quality and health benefits from fleet electrification in China. Nat Sustain 2019;2(10):962–71. http://dx.doi.org/10.1038/s41893-019-0398-8.

[6] BNEF. Electric vehicle outlook 2019. Report, New York, NY: Bloomberg New Energy Finance; 2019.

[7] Islam A, Lownes N. When to go electric? A parallel bus fleet replacement study. Transp Res D 2019;72:299–311. http://dx.doi.org/10.1016/j.trd.2019.05.007.

[8] Pelletier S, Jabali O, Mendoza JE, Laporte G. The electric bus fleet transition problem. Transp Res C 2019;109:174–93. http://dx.doi.org/10.1016/j.trc.2019.10.012.

[9] Staffell I, Scamman D, Velazquez Abad A, Balcombe P, Dodds PE, Ekins P, et al. The role of hydrogen and fuel cells in the global energy system. Energy Environ Sci 2019;12(2):463–91. http://dx.doi.org/10.1039/c8ee01157e.

[10] Dunn JB, Newes E, Cai H, Zhang Y, Brooker A, Ou L, et al. Energy, economic, and environmental benefits assessment of co-optimized engines and bio-blendstocks. Energy Environ Sci 2020. http://dx.doi.org/10.1039/d0ee00716a.

[11] Plötz P, Axsen J, Funke SA, Gnann T. Designing car bans for sustainable transportation. Nat Sustain 2019;2(7):534–6. http://dx.doi.org/10.1038/s41893-019-0328-9.

[12] Nordhaus W. Climate change: The ultimate challenge for economics. Amer Econ Rev 2019;109(6):1991–2014. http://dx.doi.org/10.1257/aer.109.6.1991.

[13] Luderer G, Vrontisi Z, Bertram C, Edelenbosch OY, Pietzcker RC, Rogelj J, et al. Residual fossil CO_2 emissions in 1.5-2° C pathways. Nature Clim Change 2018;8(7):626–33. http://dx.doi.org/10.1038/s41558-018-0198-6.

[14] de Chalendar JA, Glynn PW, Benson SM. City-scale decarbonization experiments with integrated energy systems. Energy Environ Sci 2019;12:1695–707. http://dx.doi.org/10.1039/C8EE03706J.

[15] Lebeau P, Macharis C, Mierlo J, Lebeau K. Electrifying light commercial vehicles for city logistics? A total cost of ownership analysis. Eur J Transp Infrastruct Res 2015;15(4). http://dx.doi.org/10.18757/ejtir.2015.15.4.3097.

[16] Lajunen A, Lipman T. Lifecycle cost assessment and carbon dioxide emissions of diesel, natural gas, hybrid electric, fuel cell hybrid and electric transit buses. Energy 2016;106:329–42. http://dx.doi.org/10.1016/j.energy.2016.03.075.

[17] Feng W, Figliozzi M. An economic and technological analysis of the key factors affecting the competitiveness of electric commercial vehicles: A case study from the USA market. Transp Res C 2013;26:135–45. http://dx.doi.org/10.1016/j.trc.2012.06.007.

[18] Ansaripoor AH, Oliveira FS, Liret A. Recursive expected conditional value at risk in the fleet renewal problem with alternative fuel vehicles. Transp Res C 2016;65:156–71. http://dx.doi.org/10.1016/j.trc.2015.12.010.

[19] Tong F, Hendrickson C, Biehler A, Jaramillo P, Seki S. Life cycle ownership cost and environmental externality of alternative fuel options for transit buses. Transp Res D 2017;57:287–302. http://dx.doi.org/10.1016/j.trd.2017.09.023.

[20] Borlaug B, Salisbury S, Gerdes M, Muratori M. Levelized cost of charging electric vehicles in the United States. Joule 2020;4(7):1470–85. http://dx.doi.org/10.1016/j.joule.2020.05.013.

[21] Ahani P, Arantes A, Melo S. A portfolio approach for optimal fleet replacement toward sustainable urban freight transportation. Transp Res D 2016;48:357–68. http://dx.doi.org/10.1016/j.trd.2016.08.019.

[22] López-Ibarra JA, Gaztañaga H, de Ibarra AS, Camblong H. Plug-in hybrid electric buses total cost of ownership optimization at fleet level based on battery aging. Appl Energy 2020;280:115887. http://dx.doi.org/10.1016/j.apenergy.2020.115887.

[23] Shea RP, Worsham MO, Chiasson AD, Kelly Kissock J, McCall BJ. A lifecycle cost analysis of transitioning to a fully-electrified, renewably powered, and carbon-neutral campus at the University of Dayton. Sustain Energy Technol Assess 2020;37:100576. http://dx.doi.org/10.1016/j.seta.2019.100576.

[24] Cooper R, Kaplan RS. Activity-based systems: Measuring the costs of resource usage. Harv Bus Rev 1992;6(3):96–103.

[25] Kaplan RS, Anderson SR. Time-driven activity-based costing: a simpler and more powerful path to higher profits. Harvard Business Press; 2007.

[26] Glenk G, Reichelstein S. Synergistic value in vertically integrated power-to-gas energy systems. Prod Oper Manage 2020;29(3):526–46. http://dx.doi.org/10.1111/poms.13116.

[27] Harris A, Soban D, Smyth BM, Best R. A probabilistic fleet analysis for energy consumption, life cycle cost and greenhouse gas emissions modelling of bus technologies. Appl Energy 2020;261:114422. http://dx.doi.org/10.1016/j.apenergy.2019.114422.

[28] Johnson C, Nobler E, Eudy L, Jeffers M. Financial analysis of battery electric transit buses. Tech. rep. NREL/TP-5400-74832, Golden, CO.: National Renewable Energy Laboratory (NREL); 2020, URL: https://www.nrel.gov/docs/fy20osti/74832.pdf.

[29] APTA. 2019 Public transportation fact book. Report 70th edition, Washington DC: American Public Transportation Association; 2019.

[30] The European Commission. Clean vehicles directive. 2019, URL: https://ec.europa.eu/transport/themes/urban/clean-vehicles-directive_en.

[31] MIT. The future of coal: Options for a carbon-constrained world. Tech. rep., Cambridge, MA: Massachusetts Institute of Technology; 2007.

[32] Reichelstein S, Rohlfing-Bastian A. Levelized product cost: Concept and decision relevance. Account Rev 2015;90(4):1653–82. http://dx.doi.org/10.2308/accr-51009.

[33] Comello S, Reichelstein S. The emergence of cost effective battery storage. Nature Commun 2019;10(1):2038. http://dx.doi.org/10.1038/s41467-019-09988-z.

[34] CARB. Hybrid and zero-emission truck and bus voucher incentive project. 2020, URL: https://www.californiahvip.org/how-to-participate/#Eligible-Vehicle-Catalog.

[35] Schmidt TS, Steffen B, Egli F, Pahle M, Tietjen O, Edenhofer O. Adverse effects of rising interest rates on sustainable energy transitions. Nat Sustain 2019;2(9):879–85. http://dx.doi.org/10.1038/s41893-019-0375-2.

[36] Baumgarte F, Glenk G, Rieger A. Business models and profitability of energy storage. iScience 2020;23(10):101554. http://dx.doi.org/10.1016/j.isci.2020.101554.

[37] Schmidt O, Hawkes A, Gambhir A, Staffell I. The future cost of electrical energy storage based on experience rates. Nat Energy 2017;6(July):17110. http://dx.doi.org/10.1038/nenergy.2017.110.

[38] Nykvist B, Nilsson M. Rapidly falling costs of battery packs for electric vehicles. Nature Clim Change 2015;5(4):329–32. http://dx.doi.org/10.1038/nclimate2564.

[39] Jiao N, Evans S. Business models for repurposing a second-life for retired electric vehicle batteries. In: Pistoia G, Liaw B, editors. Behaviour of lithium-ion batteries in electric vehicles: battery health, performance, safety, and cost. Cham: Springer International Publishing; 2018, p. 323–44. http://dx.doi.org/10.1007/978-3-319-69950-9_13.

[40] Martinez-Laserna E, Gandiaga I, Sarasketa-Zabala E, Badeda J, Stroe D-I, Swierczynski M, Goikoetxea A. Battery second life: Hype, hope or reality? A critical review of the state of the art. Renew Sustain Energy Rev 2018;93:701–18. http://dx.doi.org/10.1016/j.rser.2018.04.035.

[41] Schmidt O, Melchior S, Hawkes A, Staffell I. Projecting the future levelized cost of electricity storage technologies. Joule 2019;3(1):81–100. http://dx.doi.org/10.1016/j.joule.2018.12.008.

[42] Stanford University. Historical utilities rates - charge out rates. 2020, URL: https://lbre.stanford.edu/sem/historical-utilities-rates.

[43] Eudy L, Prohaska R, Kelly K, Post M. Foothill transit battery electric bus demonstration results. Report NREL/TP-5400-65274, Golden, CO: National Renewable Energy Laboratory; 2016.